Virology 505 (2017) 172–180

Contents lists available at ScienceDirect

Virology

journal homepage: www.elsevier.com/locate/yviro

Active and separate secretion of fiber and penton base during the early phase of Ad2 or Ad5 infection

Yuhua Yan[a,1], Bo Zhang[a,1], Weihong Hou[a], Hongyu Lin[a], Johan Rebetz[b], Saw-See Hong[c], Youjun Wang[a], Liang Ran[a], Xiaolong Fan[a,*]

[a] Beijing Key Laboratory of Gene Resource and Molecular Development, Beijing Normal University, Beijing, China
[b] The Rausing Laboratory, Department of Neurosurgery, Lund University, Lund, Sweden
[c] Viral Infections & Comparative Pathology, UMR-754 UCBL-INRA-EPHE, Université Lyon 1, Lyon Cedex 07, France

ARTICLE INFO

Keywords:
Adenovirus
Fiber protein
Penton base
Secretion

ABSTRACT

Fiber and penton base overproduced in adenovirus (Ad) infected cells can be secreted prior to progeny release and thereby regulate progeny spread. We aimed to investigate the mechanisms of fiber and penton base secretion in Ad2- or Ad5-infected A549 cells. Our flow cytometry analyses detected abundant surface fiber molecules, but little penton base molecules at 12 h post infection. Immunogold staining combined with transmission electron microscopic analyses revealed separate, non-co-localized release of fiber and penton base in the proximity of the plasma membrane. Depolymerization of microtubule and actin cytoskeletons, and inhibition of Rock kinase and myosin II activity together demonstrated cytoskeletal network-dependent fiber secretion. Inhibition of intracellular calcium $[Ca^{2+}]_i$ signaling caused diminished fiber secretion, which was associated with diminished progeny production. Thus, fiber and penton base are actively and separately secreted during the early stages of Ad2 or Ad5 infection, their secretion may play important role in Ad life cycle.

1. Introduction

Adenoviruses (Ad) infections, causing a variety of diseases in respiratory, ocular and enteric systems, are common in human populations. Currently, 70 human Ad types classified in seven species are recognized (Hage et al., 2015). While the majority of Ad types cause mild, subclinical infections, Ad subtypes of species B, D and F often cause severe or even life threating infections. Factors regulating the difference in tropism and virulence among various types of Ads are not completely understood.

Ads are non-enveloped virions with a capsid surrounding the 36-kb linear double-stranded DNA genome and associated DNA binding proteins. The capsid contains three major structural proteins, the hexon, the fiber and the penton base. Ad infection in many host cells is initiated by the attachment of the fiber knob domain to the corresponding receptor of the host cell. The penton base molecules subsequently interact with the cellular integrins (Wickham et al., 1993) and this promotes viral internalization, fusion with endosomal membranes and trafficking via the endocytic pathway (Meier et al., 2002; Nemerow and Stewart, 1999). While fiber molecules from the majority of Ad types bind to the Coxsackievirus and Adenovirus Receptor (CAR) (Bergelson et al., 1997), fiber molecules of species B Ads bind either to CD46 (Gaggar et al., 2003; Segerman et al., 2003), or Desmoglein 2 (Wang et al., 2011), fiber molecules of Ad37 bind to GD1a glycan (Nilsson et al., 2011).

In Ad infected cells, fiber and penton base are produced in large excess relative to the needs of Ad particle assembly (Fender et al., 2012; Franqueville et al., 2008; Lu et al., 2013; Norrby, 1969). Recent studies suggest that the free structural proteins may play important roles in Ad life cycle and Ad pathogenesis. High concentrations of fiber may function as a platform for the assembly of Ad particles in Ad5 infected cells (Franqueville et al., 2008). Using polarized epithelial cells, free fiber molecules released from Ad5 infected cells and penton-dodecahedral particles are suggested to open up intercellular junctions and thereby support the spread of progeny viruses (Fender et al., 2012; Lu et al., 2013; Walters et al., 2002). Our previous studies, though limited to non-polarized cells, suggest that the release of fiber molecules from Ad infected cells can cause receptor masking in the adjacent cells and thereby protect these cells from infection with the progeny virus (Rebetz et al., 2009).

Mechanisms for the release of fiber and penton base molecules from Ad infected cells prior to the release of progeny virus remain currently unknown. Signaling sequences directing newly synthesized peptides to

* Corresponding author.
E-mail address: XFan@bnu.edu.cn (X. Fan).
[1] These authors contributed equally to this work.

http://dx.doi.org/10.1016/j.virol.2017.02.018
Received 21 October 2016; Received in revised form 23 January 2017; Accepted 22 February 2017

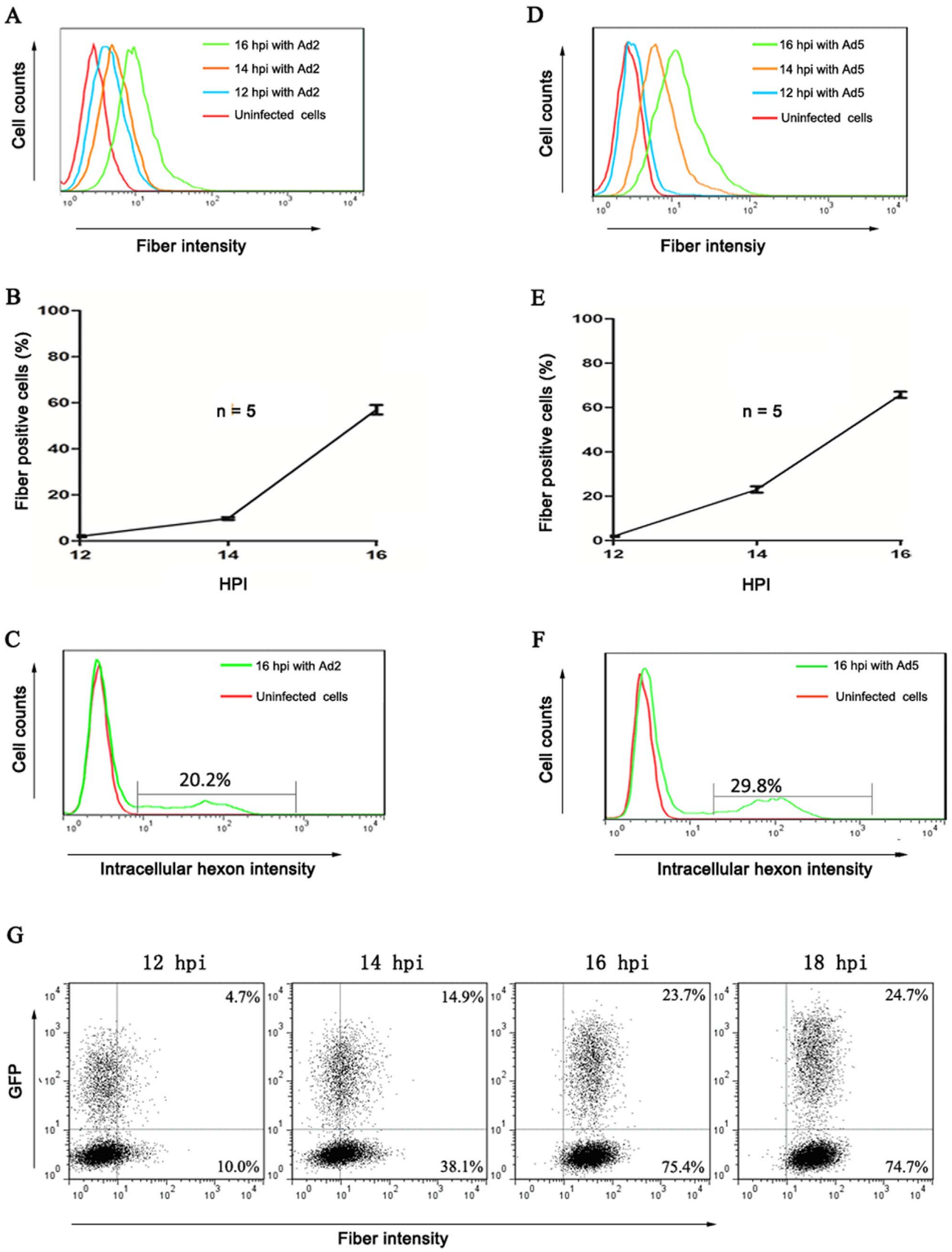

Fig. 1. Time course of fiber secretion in cells following infection with Ad2 or Ad5 viruses. A549 cells were infected by Ad2 (A, B and C) or Ad5 (D, E and F) at a MOI of 50. Cell surface binding of fiber was measured using flow cytometry analysis at 2 h intervals. From 12 hpi, increasing intensity (A and D) and proportion of cells (B and E) with surface fiber binding were detected. At 16 hpi, less than 30% of the total cells showed intracellular hexon staining (C and F). Dot-plots in panel **G** depict representative results of GFP expression and surface fiber staining in 293 cells at the indicated times following infection with Ad5-GFP vector at a MOI of 5.

the endoplasmic reticulum are not encoded in the mRNA either of the fiber or of the penton base. Consequently, as previously reported in transfection studies using plasmids encoding Ad2 fiber or penton base or after infection with Ad2 or Ad5 viruses, these molecules can not be secreted via the Golgi-dependent classical export machinery (Trotman et al., 2003). In addition, penton base was found to be secreted in an autonomous fashion in Ad2 or Ad5 infected cells; whereas fiber secretion was found to be dependent on the release of penton base (Trotman et al., 2003). However, the conclusion that secretion of penton base is autonomous while the secretion of fiber is penton base-dependent was largely based on the assessment of their spreading patterns at relatively late phases of Ad2 infection (Trotman et al., 2003). Whether, and if so how, fiber molecules could be released during the early phase of Ad2 infection is so far unclear.

In this report, we have studied the secretion kinetics of fiber and penton base in the early phases of Ad2 and Ad5 infection. Using flow cytometry analysis, we show that early in Ad2 or Ad5 infection, fiber is secreted prior to the secretion of penton base. Our transmission electron microscopy (TEM) analyses of the fiber and penton base immunostaining show that fiber and penton base molecules are separately secreted at the plasma membrane. The secretion of fiber molecules is dependent on the cytoskeletal network, and can be inhibited by inhibitors of myosin II motor protein, of ROCK kinase and of intracellular Ca^{2+} signaling.

2. Materials and methods

2.1. Viruses used in this study

The wild-type Ad2 and Ad5 were kindly provided by Dr. Niklas Arnberg. The Ad5-GFP vector was an E1-deleted recombinant Ad vector with a GFP expression cassette engineered in the E1 region (Nilsson et al., 2004). Ad2 and Ad5 were expanded in A549 cells, and Ad5-GFP in 293 cells. Viruses were prepared by two-step CsCl gradient centrifugation. Physical particle titer was measured at OD_{260} (Mittereder et al., 1996). We have considered a ratio of 50:1 between the physical particles and infectious unit.

2.2. Cell culture and inhibitor treatment

A549 or 293 cells were cultured in DMEM supplemented with 10% heat inactivated fetal bovine serum, 100 U/ml penicillin and 100 μg/ml streptomycin. Cells were seeded at 2×10^5 cells/well in 12-well plates. Five hours later, cells were infected with Ad in 0.4 ml medium containing 2% fetal bovine serum. Unbound virus was removed by twice washing at 2 hpi and cells were then cultured with 0.4 ml medium containing 2% fetal bovine serum. For the cytoskeleton inhibition studies, cells were treated with nocodazole (Sigma) or latrunculin B (Sigma) at the indicated concentration between 12 and 14 hpi. To detect whether 293 cell cultures at 18 hpi with Ad5-GFP infection contained lysed cells, the supernatants of 293 cells cultured in 12-well plates were transferred well-by-well to A549 cells cultured in 12-well plates. No GFP positive cells were detected by fluorescence microscopy over the course of 72 h of incubation. For myosin II inhibition studies, cells were treated with Y27632 (Selleckchem) or blebbistatin (Sigma) at the indicated concentrations from 12 to 16 hpi. For chelation of $[Ca^{2+}]_i$, cells were treated with BAPTA-AM (Sigma) at the indicated concentration between 12 and 14 hpi. For chelation of the extracellular Ca^{2+} pool, cells were cultured in DMEM without calcium

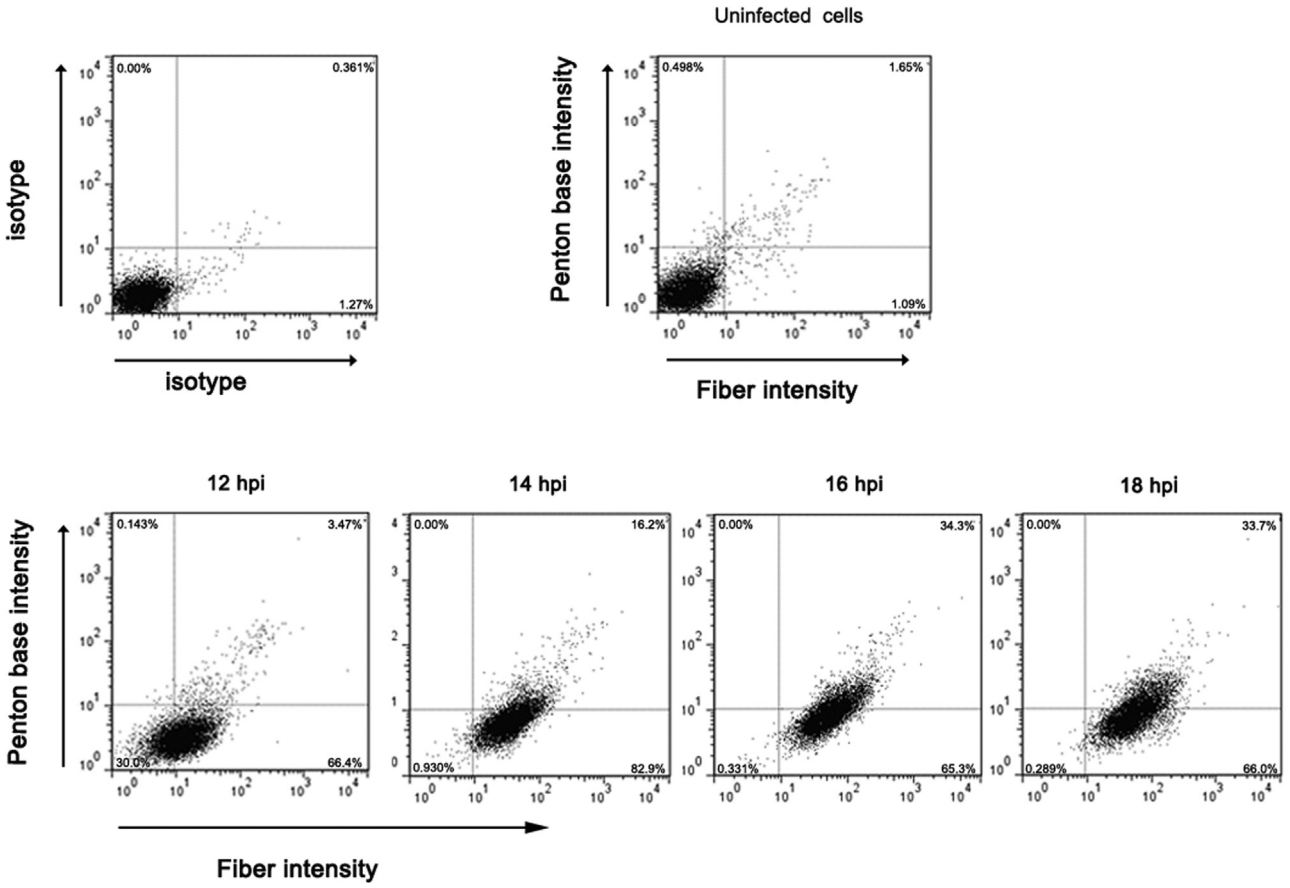

Fig. 2. Different secretion kinetics of fiber and penton base in A549 cells infected by Ad2 viruses. A549 cells infected by Ad2 at a MOI of 50 were co-stained for surface binding of fiber and penton base at the indicated time points post infection. Most of the cells showed surface fiber staining at 14 hpi, when surface staining of penton bases started to be detectable. From 18 hpi, the majority of the cells showed surface staining of both fiber and penton base. Dot-plots of fiber and penton base staining representative of 3 experiments are shown. The percentages of cells positively stained with fiber or penton base are indicated in the quadrates of each dot plot. Similar data were observed in Ad5 infected A549 cells as shown in Fig. S1.

and treated with EGTA (Sigma) at 0.5 or 1 mM from 12 to 16 hpi.

2.3. Flow cytometry analysis

Cell surface binding of fiber, penton base or hexon was assessed at 12, 14, 16, 18 hpi. In all experiments for staining of the surface binding of adenoviral proteins, incubations with antibody were performed on ice. Following titration of the antibodies, saturating amounts of the antibodies at concentrations without inducing non-specific staining in the non-infected cells were used. For staining of fiber, cells were first incubated with mouse anti-fiber antibody (mAb 4D2, 1:200, Abcam) for 15 min. Following two washes with PBS containing 2% FCS, cells were incubated with Alexa Fluor 647 conjugated goat anti-mouse IgG (at 1:200 dilution, Life Technologies). For staining of hexon, cells were incubated with FITC conjugated goat anti-hexon antibody (at 1:200 dilution, Millipore). For co-staining of fiber and penton base, cells were first incubated with mouse anti-fiber antibody (mAb 4D2, 1:200) and rabbit anti-penton base antibody (at 1:1000 dilution) for 15 min. Subsequently, cells were washed and incubated with the Alexa Fluor 647 conjugated goat anti-mouse IgG (at 1:200 dilution, Life Technologies) and Alexa Fluor 488 conjugated goat anti-rabbit IgG (at 1:200 dilution, Life Technologies). Finally, washed cells were resuspended in PBS containing 1 μg/ml 7-aminoactinomycin (7-AAD, Sigma). Cell surface binding of fiber, penton base or hexon was analyzed in living cells negatively stained with 7-AAD. For the isotype staining of the infected cells as control, infected cells at the indicated time points post infection were first incubated with mouse IgG2a κ isotype control antibody (at 1:200 dilution, BD Biosciences) for 15 min. Following two washes with PBS containing 2% FCS, cells were incubated with Alexa Fluor 647 or Alexa Fluor 488 conjugated goat anti-mouse IgG (at 1:200 dilution, Life Technologies) and analyzed in flow cytometry.

Quantification of the total fiber and hexon molecules in infected cells was performed using Cytofix/Cytoperm™ Kit (BD 554714). Cells were first treated with BD Cytofix/Cytoperm solution. The BD Perm/Wash solution was used to wash the cells and to dilute the anti-fiber or anti-hexon antibodies. For staining of fiber, cells were incubated with the 4D2 anti-fiber antibody at 1:200 dilution for 25 min. Following two washes with the BD Perm/Wash solution, cells were incubated with Alexa Fluor 647 conjugated goat anti-mouse IgG at 1:200 dilution in the BD Perm/Wash solution, For staining of hexon, cells were incubated with FITC conjugated goat anti-hexon antibody at 1:200 dilution. Finally, cells were twice washed with the BD Perm/Wash solution, re-suspended in PBS, and analyzed by flow cytometry.

2.4. Immmunogold labeling and TEM analysis of fiber and penton base in Ad2 or Ad5 infected cells

A549 cells at 16 or 20 hpi with Ad2 at a MOI of 50 were harvest and then fixed in 4% paraformaldehyde and 0.5% glutaraldehyde in 0.1 M phosphate buffer (PB, pH 7.4) for 2 h at 4 °C. After three washes in PB, fixed cells were successively dehydrated in 30% ethanol for 20 min, 50% ethanol for 20 min, and 70%, 90% and 100% ethanol for 15 min each. Thereafter the fixed cells were treated with a mixture containing 50% LR white and 50% ethanol for 1 h, 75% LR white and 25% ethanol mixture for 1 h, 100% LR white first for 1 h, and then overnight. Samples were subsequently embedded in fresh LR white resin in gelatin capsules, and polymerized at 50 °C for at least 24 h. The specimen blocks were sliced into 60 nm ultrathin sections and loaded on 100-mesh nickel grids.

Double immunogold labeling was used to detect fiber and penton base in the ultrathin sections. The sections were first blocked with 2% BSA and 2% fetal calf serum for 1 h at room temperature, followed by incubation with anti-fiber mAb 4D2 (at 1:50 dilution in 1% BSA) overnight at 4 °C. The grids were then washed by flotation on fresh droplets of PBS for 30 min with 5 changes of PBS. Binding of 4D2 was detected with donkey anti mouse IgG conjugated with 6 nm-colloidal gold particles (1:25, Jackson Laboratory) for 1 h at room temperature. After another 5 washing steps in PBS, the same sections were incubated with anti-penton base polyclonal antibody (1:1000) and donkey anti rabbit IgG conjugated with 12 nm-colloidal gold particles (1:25, Jackson Laboratory). The stained sections were then counterstained with uranyl acetate before examination. Control stainings omitting the primary antibodies were performed in parallel, and showed no specific staining of the colloidal gold particle-conjugated secondary antibodies. The sections were examined in a TECNAI G2 Spirit transmission electron microscope.

2.5. Measurements of intracellular Ca^{2+}

Measurements of $[Ca^{2+}]_i$ were performed using the Ca^{2+} indicator FURA-2 (Sigma). Loading of FURA-2/AM and measurement of FURA-2 fluorescence were performed according to the procedure described by Mancarella et al. (2011). Semi-confluent A549 cells were cultured on coverslips in 6-well plates. After 6 h, cells were infected with Ad2 at a MOI of 50. At 16 hpi, cells grown on coverslips were placed in Imaging Bath Solution (107 mM NaCl, 7.2 mM KCl, 1.2 mM MgCl2, 11.5 mM glucose, 20 mM Hepes-NaOH, 0.1% BSA, pH 7.2) with 1 mM Ca^{2+} and

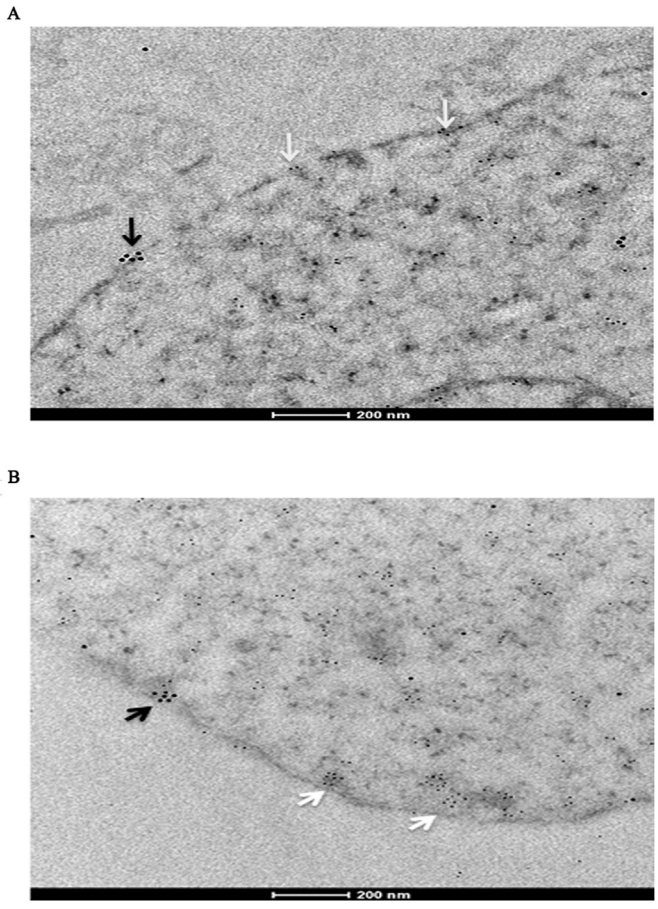

Fig. 3. Separate secretion of fiber and penton base in A549 cells at the early phase of Ad2 infection. A549 cells were infected by Ad2 at a MOI of 50. At 16 or 20 hpi, cells were harvested, fixed with paraformaldehyde and glutaraldehyde, and subsequently dehydrated and embedded for preparation of ultrathin sections. These sections were co-stained with the primary antibodies against fiber or penton base and then with the secondary antibodies conjugated with 6 nm-colloidal gold particles (for detection of fiber), or with 12 nm-colloidal gold particles (for detection of penton base). Following negative staining, the sections were observed in TECNAI G2 Spirit TEM. Separate secretion of fiber and penton base from plasma membrane was observed in cells at both 16 (A) and 20 (B) hpi. The white arrows indicate fiber molecules and the black arrows indicate penton base molecules.

loaded with FURA-2/AM (2 μM) for 30 min at room temperature. The coverslips were then transferred to FURA-2-free Imaging Bath Solution containing 1 mM Ca^{2+} for a further 30 min to wash out extracellular FURA-2/AM and to allow for intracellular cleavage of FURA-2/AM to FURA-2. The coverslip with cells was then placed in a perfusion chamber on the stage of Zeiss AX10 Observer A1, which was equipped with LAMBDA DG4 ultra-high-speed wavelength system and controlled by MetaFluor software (version 7.7.4.0, Molecular Devices). Fluorescence emission at 510 nm was monitored while alternating excitation wavelengths between 340 and 380 nm at a frequency of 0.5 Hz, $[Ca^{2+}]_i$ measurements are shown as 340:380 nm ratio from groups of at least 10 cells. The Image Bath Solution containing 1 mM Ca^{2+} was then replaced with Calcium free Imaging Bath Solution. After about 50 s delay, ionomycin (Sigma) at 2.5 μM dissolved in Calcium free imaging bath solution was added to the chamber. A subsequent increase in the ratio of fluorescence emission exited at 340/380 nm shows a relative change in cytosolic $[Ca^{2+}]_i$. Representative traces of at least three independent repeats are shown in Fig. 6 as mean ± SEM.

3. Results

3.1. Different kinetics of fiber and penton base secretion in cells infected by Ad2 or Ad5 viruses

We first assessed the time course of fiber and penton base secretion in adenocarcinoma lung cancer A549 cells following infection with Ad2 or Ad5 at a multiplicity of infection (MOI) of 50. Because hexon protein is not separately secreted (Trotman et al., 2003), surface hexon staining indicates the presence of progeny viral particles released after lysis of infected cells. Under our experimental conditions, increasing hexon

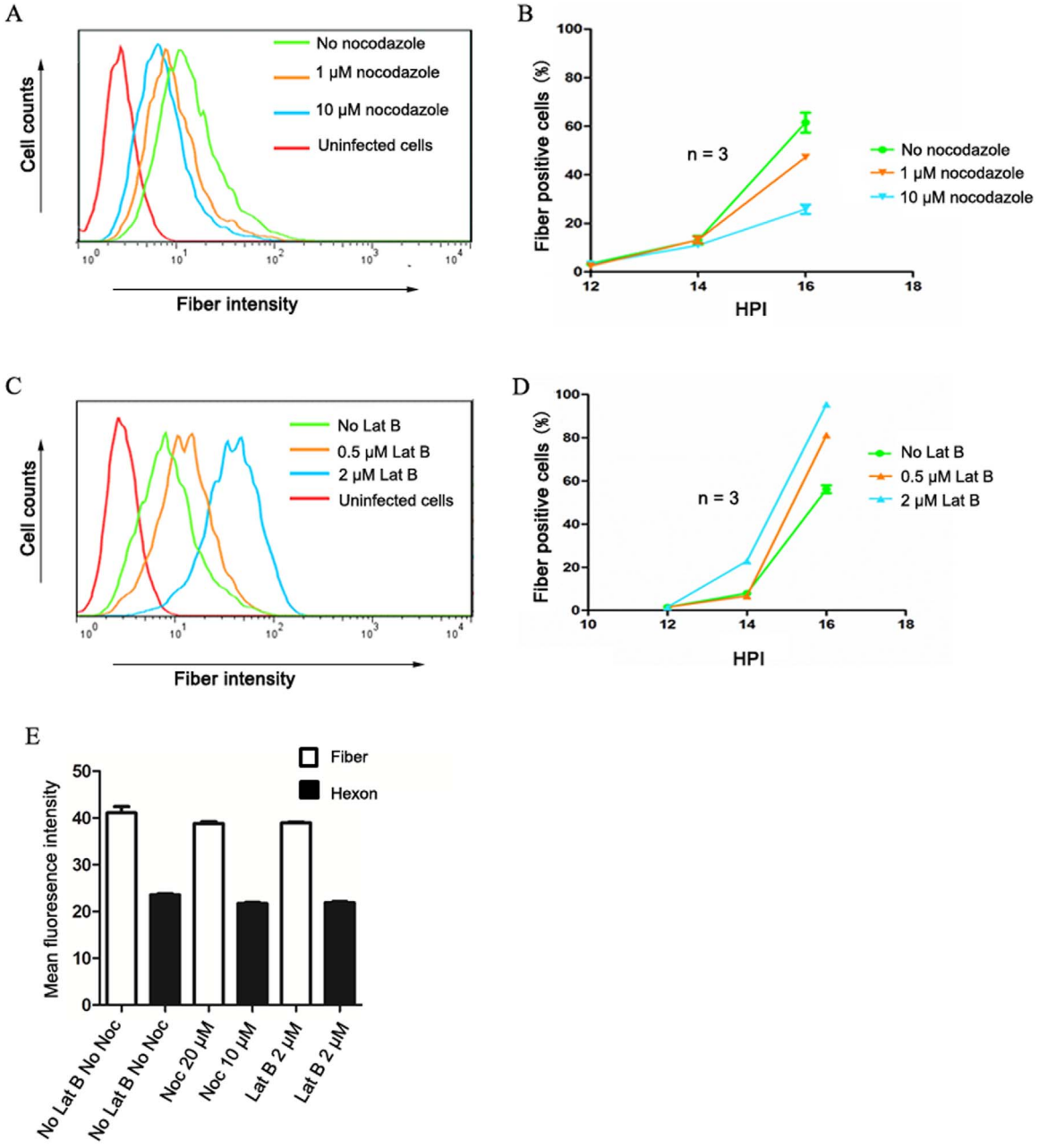

Fig. 4. Involvement of cytoskeleton network in fiber secretion. A549 cells infected with Ad2 at a MOI of 50 were treated between 12 and 14 hpi with nocodazole (A and B) or Lat B (C and D) at the indicated concentrations. Surface fiber intensity was measured at 16 hpi. Plots of representative histograms of fiber intensity (A and C) and the percentages of cells with surface fiber from three replicated experiments (B and D) are shown. Treatment with nocodazole or Lat B did not inhibit the general expression of fiber and hexon as measured by the intracellular intensities of hexon and fiber (E) in Ad2 infected A549 cells.

staining was detected on the surface of A549 cells after 18–20 hpi.

We therefore focused our analysis of surface fiber staining prior to the appearance of increased surface hexon binding. Increasing intensities and frequencies of cells with surface fiber binding were detected from 12 hpi (Figs. 1A and 1D). At 16 hpi, about 60% of the cells showed strong surface fiber binding (Figs. 1B and 1E). Intracellular hexon staining, detectable in about 10% and 14% of the total cells at 12 and 14 hpi, respectively, was detected in no more than 30% of the total cells at 16 hpi (Figs. 1C and 1F), suggesting that surface fiber molecules on the majority of the cells were derived from the bystander cells expressing hexon. We also tested if fiber molecules were present in the extracellular medium. Nearly confluent A549 cells grown on transwell membrane filters with pore size of 3.0 μm were placed into the medium recovered from cultures of A549 cells 12 and 16 hpi with Ad2. Fiber binding to the cells on the transwell filters was not detected. Thus, fiber molecules secreted from the infected cells appeared to bind rapidly to the cell surface without an extended period in the extracellular medium. Early fiber secretion was similarly shown in 293 cells (Fig. 1**G**) following infection with an Ad5-GFP vector at a MOI of 5. At 18 hpi, fiber was detected on the surface of both infected cells (about 25% of the total cells) and non-infected cells. No GFP expressing cells were detected in A549 cultures following an incubation of 72 h with the supernatant of 293 cell cultures harvested at 18 hpi with Ad5-GFP vector, indicating that surface fiber molecules detected before 18 hpi were unlikely to be derived from the lysis of infected cells.

Co-staining of fiber and penton base in Ad2 or Ad5 infected A549 cultures with saturating amounts of the antibodies showed that surface binding of penton base followed delayed kinetics compared to fiber. At 12 hpi, less than four percent of the total cells showed barely detectable surface binding of penton base whereas fiber binding was detected on the majority of the cells. Surface binding of penton base increased during the course of the subsequent infection, with about 34% of the total cells showing surface penton base at 18 hpi (Fig. 2). Similar time courses for the surface binding of fiber and penton base were detected in A549 cell cultures infected by Ad5 (Fig. S1). These findings are consistent with previous results on the early secretion of fiber molecules (Rebetz et al., 2009), but indicate that the secretion of fiber molecules in cells infected by Ad2 or Ad5 is not necessarily dependent on the expression of penton base.

3.2. Separate secretion of fiber and penton base molecules in Ad2 infected cells

To directly visualize the secretion of fiber and penton base, transmission electron microscopy (TEM) analysis in combination with immunogold staining of fiber and penton base was performed in Ad2 infected A549 cultures at 16 or 20 hpi. Ultrathin sections of the cells fixed with paraformaldehyde and glutaraldehyde were co-stained with the same anti-fiber and anti-penton base primary antibodies used in the flow cytometry analyses. The binding of the anti-fiber 4D2 mAb was visualized with secondary antibodies conjugated with 6 nm-colloidal gold particles, whereas the binding of the anti-penton base antibodies was visualized with secondary antibody conjugated with 12 nm-colloidal gold particles. Multiple replications with A549 cultures following Ad2 infection were performed. Close localization of fiber and penton base molecules was observed in the nucleus of Ad2 infected cells **(**Fig. S4A**)**. In the cytoplasm, fiber and penton base molecules were not closely located, instead concentrated in separate "granules" **(**Fig. S4B**)**. The nature of these "granules", with lysosome-like morphology, requires further investigation. We focused our analysis of fiber and penton base staining to the proximity of the plasma membrane. At both 16 and 20 hpi, separate secretion of fiber and penton base molecules was detected, co-localization of fiber and penton base was not observed (Figs. 3A and 3B).

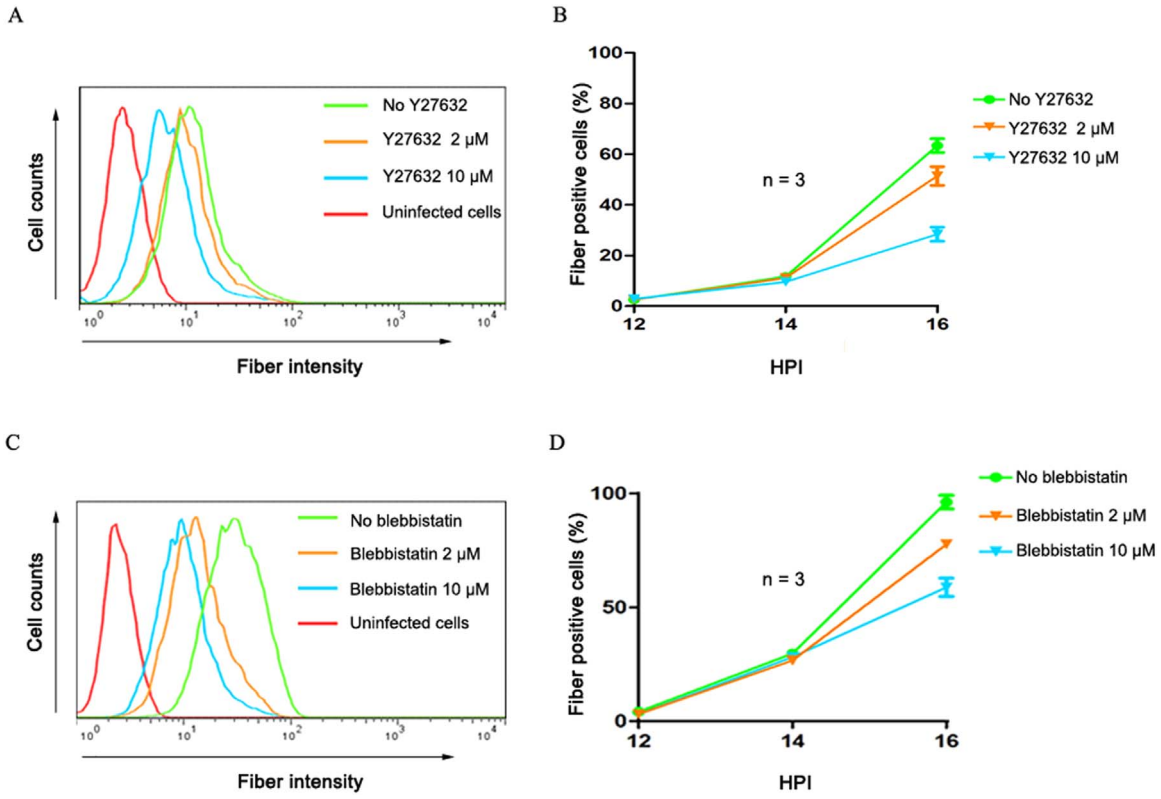

Fig. 5. Requirement of myosin II activity for fiber secretion. A549 cells infected by Ad2 at a MOI of 50 were treated with Y27632 (A and B) or blebbistatin (C and D) at the indicated concentrations starting from 12 hpi. Representative histograms of surface fiber intensity (A and C) at 16 hpi and summary of the percentages of cells with surface fiber binding at 14 or 16 hpi following Y27632 or blebbistatin treatment (B and D) are shown. Both Y27632 and blebbistatin inhibited fiber secretion in a dose-dependent manner.

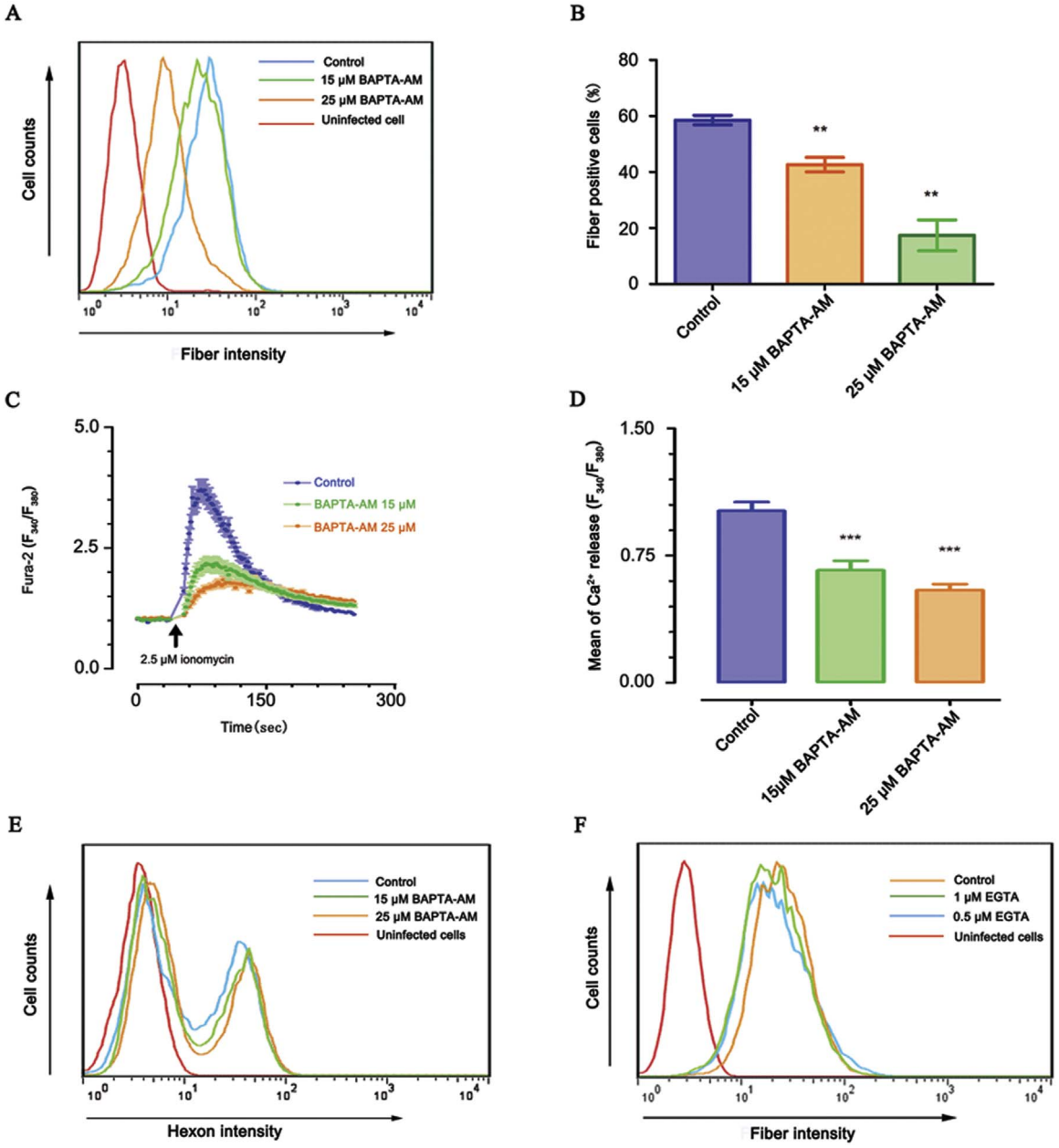

Fig. 6. Involvement of intracellular Ca^{2+} signaling in fiber secretion in Ad2 infected A549 cells. A549 cells were infected with Ad2 at a MOI of 50 and treated with BAPTA-AM between 12 and 14 hpi. Surface fiber intensities were measured at 14 and 16 hpi using flow cytometry. Representative histogram of the surface fiber binding (at 16 hpi) and the summary of the percentages of the cells with surface fiber binding are shown in (A) and (B), respectively; **: $p < 0.01$. $[Ca^{2+}]_i$ was measured with fluorescence microscopy using FURA-2-AM (C). The change in the fluorescence emission exited at 340/380 nm represents the change in $[Ca^{2+}]_i$. And summary of the mean of $[Ca^{2+}]_i$ release is shown in (D), ***: $p < 0.001$. Data show that the increase in $[Ca^{2+}]_i$ induced by ionomycin was inhibited by BAPTA-AM pre-incubation. Treatment with BAPTA-AM did not inhibit the general expression of hexon as measured by the intracellular intensity of hexon (E) in Ad2 infected A549 cells. Control experiments show that treatment with EGTA to chelate extracellular Ca^{2+} between 12 and 16 hpi did not affect fiber secretion (F).

3.3. Involvement of cytoskeleton network in fiber secretion

The above findings indicate that fiber and penton base molecules are actively secreted during the early infection of Ad2 or Ad5. To substantiate these observations, we applied several inhibitors to perturb trafficking along the cytoskeleton and assessed their effects on fiber secretion using flow cytometry analysis. We first treated Ad2 infected A549 cells with microtubule depolymerization agent nocodazole between 12 and 14 hpi, and measured the surface fiber intensity between 12 and 16 hpi. Nocodazole treatment resulted in a dose-dependent reduction of both the surface fiber intensity and the percentage of cells with bound surface fiber (Figs. 4A and 4B). However, treatment with actin depolymerization agent latrunculin B (Lat B) resulted in enhanced secretion of fiber molecules in a dose-dependent manner (Figs. 4C and 4D). We also performed fiber and hexon staining in Ad2 infected A549 cultures treated with nocodazole or Lat B following fixation and permeabilization of the cells. No measurable reduction in total fiber or hexon intensity was observed following treatment with nocodazole or Lat B in comparison with non-treated cells (Fig. 4E). Thus the alteration of the surface fiber intensity was unlikely due to an inhibition of the general fiber expression, but rather due to an altered efficiency of fiber trafficking to the cell surface.

Enhanced fiber secretion following Lat B treatment suggests depolymerization of actin network may facilitate fiber transport, which is consistent with the reports that the cortical actin cytoskeleton limits the rate and extent of vesicle exocytosis (Jog et al., 2007; Johnson

et al., 2012; Trifaro et al., 2008). Vesicles transported along the cortical actin cytoskeleton are propelled most likely by myosin II motor protein (Neco et al., 2004), because myosin V is preferentially distributed in the cell interior (Neco et al., 2002; Rose et al., 2003). Phosphorylation of myosin II light chain has been reported to facilitate the access of secretory vesicles to releasing sites along the actin network (Suzuki et al., 2006b; Trifaro et al., 2008). We therefore studied whether inhibition of myosin II phosphorylation or direct inhibition of myosin II could block fiber secretion. Rho kinase induces myosin II light chain phosphorylation via ROCK-mediated inactivation of myosin II light chain phosphatase (Maekawa et al., 1999) and thereby activates myosin II (Suzuki et al., 2006a). We first treated Ad2 infected A549 cells with the Rock kinase inhibitor Y27632 2–10 μM) between 12 and 16 hpi. A dose-dependent reduction in the intensity of surface fiber binding and percentage of cells with surface fiber binding was detected at 16 hpi. Similarly, treatment of Ad2 infected A549 cells with blebbistatin, an inhibitor of myosin II ATPase activity with high affinity and selectivity (Kovacs et al., 2004), also inhibited fiber secretion in a dose-dependent manner (Fig. 5). These results together suggested that fiber secretion was regulated by the cytoskeletal network.

3.4. Requirement of intracellular Ca^{2+} signaling for fiber secretion

Transport and exocytosis in the proximity of the plasma membrane are regulated by Ca^{2+} signaling (Neher, 1998; Trifaro et al., 2008). To assess the role of Ca^{2+} signaling in fiber secretion, we treated Ad2 infected A549 cells with BAPTA-AM to clamp the intracellular Ca^{2+} levels. Surface fiber intensity and the percentages of the cells with surface fiber staining were reduced in a BAPTA-AM dose-dependent manner (Figs. 6A and 6B). Both the surface fiber intensity and the percentages of the cells with surface fiber staining in cultures treated with 25 μM BAPTA-AM were reduced to one third compared to cultures without BAPTA-AM treatment. To confirm that the cytoplasmic Ca^{2+} level was decreased to low levels following calcium chelation by BAPTA-AM, FURA-2 experiments with the ionophore ionomycin were performed. FURA-2 measurements revealed that the ionomycin induced increase in $[Ca^{2+}]_i$ due to release of Ca^{2+} from ER stores, was inhibited by BAPTA-AM preincubation (Figs. 6C and 6D). No measureable reduction in total hexon intensity was observed following treatment with BAPTA-AM in comparison with non-treated cells (Fig. 6E). Furthermore, no alteration in surface fiber intensity was observed in Ad2 infected cells following treatment with EGTA between 12 and 16 hpi (Fig. 6F), suggesting that fiber secretion was not dependent on Ca^{2+} influx from the extracellular Ca^{2+} pool.

4. Discussion

Fiber and penton base play key roles in the initiation of Ad infection. During the infection of many Ad serotypes, fiber and penton base molecules are produced in large excess relative to the amounts required for Ad particle assembly (Franqueville et al., 2008; Fuschiotti et al., 2006; Rebetz et al., 2009; Trotman et al., 2003). Several studies, including our studies, have indicated that the secretion of fiber and penton base may result in receptor masking in bystander cells and thereby regulate the spread of Ad infection (Fender et al., 2012; Lu et al., 2013; Rebetz et al., 2009; Walters et al., 2002). Our goal was to characterize the secretion path of fiber and penton base molecules in the early phase of Ad2 or Ad5 infection. Our findings extend previous findings (Rebetz et al., 2009; Trotman et al., 2003; Walters et al., 2002) on fiber and penton base overproduction in Ad2 or Ad5 infection in the following aspects: *i*) fiber molecules are secreted earlier compared to the secretion of penton base molecules; *ii*) fiber and penton base molecules are secreted separately; *iii*) the trafficking and release of fiber, and likely also of the penton base, is dependent on the cytoskeletal network and on intracellular Ca^{2+} signaling.

In the Ad capsid, fiber and penton base are integrated in a complex. At approximately 20 hpi, hetero-oligomers of fiber-penton base are formed in the cytosol of Ad infected cells (Russell, 2000). It was previously reported that fiber secretion in a Golgi apparatus-independent manner is dependent on penton base (Trotman et al., 2003). We found that during the early phase of infection, fiber and penton base molecules are separately secreted from the plasma membrane of Ad2 or Ad5 infected cells. These findings are consistent with previous findings that fiber and penton base in Ad2 or Ad5 infected cells can not form dodecahedron (Fender et al., 1997). However, our findings do not support the notion that early in infection fiber secretion is dependent on the secretion of penton base, although we cannot exclude that this may be the case late in infection (Trotman et al., 2003). Our findings show that penton base was significantly detected on the cell surface at 14 hpi, which is not consistent with previous findings (Trotman et al., 2003). Whereas the previous findings of penton base-dependent fiber secretion were mainly based on transfection studies using plasmids encoding fiber or penton base (Trotman et al., 2003), our findings are based on infection studies with wild-type Ad2 or Ad5 viruses. Furthermore, we have characterized the detailed kinetics of fiber secretion. Our results indicate that fiber molecules are secreted prior to the secretion of penton base. This could be linked to the fact that, though both proteins are produced in excess to the need for progeny particle assembly, the expression of the fiber protein is considerably greater than that of the penton base. However, the exact mechanisms leading to the difference in the pattern of secretion of the two proteins remains to be determined.

Cell surface fiber was already detected between 12 and 14 hpi, which is much earlier than the release of progeny virus. We have focused on the characterization of fiber secretion. Our analyses of fiber secretion kinetics, depolymerization of cytoskeleton, inhibition of myosin II motor protein and Ca^{2+} signaling, and TEM observation of Ad infected cells together indicate that fiber molecules are actively secreted and propelled along the cytoskeleton highway towards the plasma membrane. In the proximity of the plasma membrane, fiber secretion is controlled by Ca^{2+} signaling. Further investigation of the nature of fiber or penton base secretion, and the applicability of our current findings to those more pathogenic Ad serotypes such as Ad3, Ad4 and Ad7 may shed light on the hitherto poorly understood factors contributing to the tropism and pathogenesis of different adenoviruses.

Acknowledgment

This work was supported by National Natural Science Foundation of China (grant 81272535). We thank Dr. Robert S. Jack for critical input on the project.

Appendix A. Supplementary material

Supplementary data associated with this article can be found in the online version at doi:10.1016/j.virol.2017.02.018.

References

Bergelson, J.M., Cunningham, J.A., Droguett, G., Kurt-Jones, E.A., Krithivas, A., Hong, J.S., Horwitz, M.S., Crowell, R.L., Finberg, R.W., 1997. Isolation of a common receptor for Coxsackie B viruses and adenoviruses 2 and 5. Science 275, 1320–1323.
Fender, P., Hall, K., Schoehn, G., Blair, G.E., 2012. Impact of human adenovirus type 3 dodecahedron on host cells and its potential role in viral infection. J. Virol. 86, 5380–5385.
Fender, P., Ruigrok, R.W., Gout, E., Buffet, S., Chroboczek, J., 1997. Adenovirus dodecahedron, a new vector for human gene transfer. Nat. Biotechnol. 15, 52–56.
Franqueville, L., Henning, P., Magnusson, M., Vigne, E., Schoehn, G., Blair-Zajdel, M.E., Habib, N., Lindholm, L., Blair, G.E., Hong, S.S., Boulanger, P., 2008. Protein crystals in Adenovirus type 5-infected cells: requirements for intranuclear crystallogenesis, structural and functional analysis. PLoS One 3, e2894.
Fuschiotti, P., Schoehn, G., Fender, P., Fabry, C.M., Hewat, E.A., Chroboczek, J., Ruigrok, R.W., Conway, J.F., 2006. Structure of the dodecahedral penton particle from human adenovirus type 3. J. Mol. Biol. 356, 510–520.
Gaggar, A., Shayakhmetov, D.M., Lieber, A., 2003. CD46 is a cellular receptor for group B

adenoviruses. Nat. Med. 9, 1408–1412.
Hage, E., Gerd Liebert, U., Bergs, S., Ganzenmueller, T., Heim, A., 2015. Human mastadenovirus type 70: a novel, multiple recombinant species D mastadenovirus isolated from diarrhoeal faeces of a haematopoietic stem cell transplantation recipient. J. Gen. Virol. 96, 2734–2742.
Jog, N.R., Rane, M.J., Lominadze, G., Luerman, G.C., Ward, R.A., McLeish, K.R., 2007. The actin cytoskeleton regulates exocytosis of all neutrophil granule subsets. Am. J. Physiol. Cell Physiol. 292, C1690–C1700.
Johnson, J.L., Monfregola, J., Napolitano, G., Kiosses, W.B., Catz, S.D., 2012. Vesicular trafficking through cortical actin during exocytosis is regulated by the Rab27a effector JFC1/Slp1 and the RhoA-GTPase-activating protein Gem-interacting protein. Mol. Biol. Cell 23, 1902–1916.
Kovacs, M., Toth, J., Hetenyi, C., Malnasi-Csizmadia, A., Sellers, J.R., 2004. Mechanism of blebbistatin inhibition of myosin II. J. Biol. Chem. 279, 35557–35563.
Lu, Z.Z., Wang, H., Zhang, Y., Cao, H., Li, Z., Fender, P., Lieber, A., 2013. Penton-dodecahedral particles trigger opening of intercellular junctions and facilitate viral spread during adenovirus serotype 3 infection of epithelial cells. PLoS Pathog. 9, e1003718.
Maekawa, M., Ishizaki, T., Boku, S., Watanabe, N., Fujita, A., Iwamatsu, A., Obinata, T., Ohashi, K., Mizuno, K., Narumiya, S., 1999. Signaling from Rho to the actin cytoskeleton through protein kinases ROCK and LIM-kinase. Science 285, 895–898.
Mancarella, S., Wang, Y., Deng, X., Landesberg, G., Scalia, R., Panettieri, R.A., Mallilankaraman, K., Tang, X.D., Madesh, M., Gill, D.L., 2011. Hypoxia-induced acidosis uncouples the STIM-Orai calcium signaling complex. J. Biol. Chem. 286, 44788–44798.
Meier, O., Boucke, K., Hammer, S.V., Keller, S., Stidwill, R.P., Hemmi, S., Greber, U.F., 2002. Adenovirus triggers macropinocytosis and endosomal leakage together with its clathrin-mediated uptake. J. Cell Biol. 158, 1119–1131.
Mittereder, N., March, K.L., Trapnell, B.C., 1996. Evaluation of the concentration and bioactivity of adenovirus vectors for gene therapy. J. Virol. 70, 7498–7509.
Neco, P., Gil, A., Del Mar Frances, M., Viniegra, S., Gutierrez, L.M., 2002. The role of myosin in vesicle transport during bovine chromaffin cell secretion. Biochem. J. 368, 405–413.
Neco, P., Giner, D., Viniegra, S., Borges, R., Villarroel, A., Gutierrez, L.M., 2004. New roles of myosin II during vesicle transport and fusion in chromaffin cells. J. Biol. Chem. 279, 27450–27457.
Neher, E., 1998. Vesicle pools and Ca2+ microdomains: new tools for understanding their roles in neurotransmitter release. Neuron 20, 389–399.
Nemerow, G.R., Stewart, P.L., 1999. Role of alpha(v) integrins in adenovirus cell entry and gene delivery. Microbiol. Mol. Biol. Rev. 63, 725–734.
Nilsson, E.C., Storm, R.J., Bauer, J., Johansson, S.M., Lookene, A., Angstrom, J., Hedenstrom, M., Eriksson, T.L., Frangsmyr, L., Rinaldi, S., Willison, H.J., Pedrosa Domellof, F., Stehle, T., Arnberg, N., 2011. The GD1a glycan is a cellular receptor for adenoviruses causing epidemic keratoconjunctivitis. Nat. Med. 17, 105–109.
Nilsson, M., Ljungberg, J., Richter, J., Kiefer, T., Magnusson, M., Lieber, A., Widegren, B., Karlsson, S., Fan, X., 2004. Development of an adenoviral vector system with adenovirus serotype 35 tropism; efficient transient gene transfer into primary malignant hematopoietic cells. J. Gene Med. 6, 631–641.
Norrby, E., 1969. The structural and functional diversity of Adenovirus capsid components. J. Gen. Virol. 5, 221–236.
Rebetz, J., Na, M., Su, C., Holmqvist, B., Edqvist, A., Nyberg, C., Widegren, B., Salford, L.G., Sjogren, H.O., Arnberg, N., Qian, Q., Fan, X., 2009. Fiber mediated receptor masking in non-infected bystander cells restricts adenovirus cell killing effect but promotes adenovirus host co-existence. PLoS One 4, e8484.
Rose, S.D., Lejen, T., Casaletti, L., Larson, R.E., Pene, T.D., Trifaro, J.M., 2003. Myosins II and V in chromaffin cells: myosin V is a chromaffin vesicle molecular motor involved in secretion. J. Neurochem. 85, 287–298.
Russell, W.C., 2000. Update on adenovirus and its vectors. J. Gen. Virol. 81, 2573–2604.
Segerman, A., Atkinson, J.P., Marttila, M., Dennerquist, V., Wadell, G., Arnberg, N., 2003. Adenovirus type 11 uses CD46 as a cellular receptor. J. Virol. 77, 9183–9191.
Suzuki, J., Jin, Z.-G., Meoli, D.F., Matoba, T., Berk, B.C., 2006a. Cyclophilin A is secreted by a vesicular pathway in vascular smooth muscle cells. Circ. Res. 98, 811–817.
Suzuki, J., Jin, Z.G., Meoli, D.F., Matoba, T., Berk, B.C., 2006b. Cyclophilin A is secreted by a vesicular pathway in vascular smooth muscle cells. Circ. Res. 98, 811–817.
Trifaro, J.M., Gasman, S., Gutierrez, L.M., 2008. Cytoskeletal control of vesicle transport and exocytosis in chromaffin cells. Acta Physiol. 192, 165–172.
Trotman, L.C., Achermann, D.P., Keller, S., Straub, M., Greber, U.F., 2003. Non-classical export of an adenovirus structural protein. Traffic 4, 390–402.
Walters, R.W., Freimuth, P., Moninger, T.O., Ganske, I., Zabner, J., Welsh, M.J., 2002. Adenovirus fiber disrupts CAR-mediated intercellular adhesion allowing virus escape. Cell 110, 789–799.
Wang, H., Li, Z.Y., Liu, Y., Persson, J., Beyer, I., Moller, T., Koyuncu, D., Drescher, M.R., Strauss, R., Zhang, X.B., Wahl, J.K., 3rd, Urban, N., Drescher, C., Hemminki, A., Fender, P., Lieber, A., 2011. Desmoglein 2 is a receptor for adenovirus serotypes 3, 7, 11 and 14. Nat. Med. 17, 96–104.
Wickham, T.J., Mathias, P., Cheresh, D.A., Nemerow, G.R., 1993. Integrins alpha v beta 3 and alpha v beta 5 promote adenovirus internalization but not virus attachment. Cell 73, 309–319.